Investigación realizada gracias al Programa de Apoyo a Proyectos de Investigación e Innovación Tecnológica (PAPIIT) de la UNAM IN117723. Agradezco a la DGAPA-UNAM la beca recibida".

Abstract

All PhD theses must have two scientific summaries/abstracts: One in Norwegian and one in English (it can be the same text). The summaries/abstracts should be up to two pages (600–1200 words) and must be included in the thesis at the time of submission. If you need assistance for the Norwegian summary, contact your supervisor/research group. As a last resort, you could use Semantix Translations (www.semantix.no). Please contact Semantix in order to get a quote.

Automatic "quotation marks" and cross-references are handled correctly for the specified language.

Add new section about results in **??**.

Preface

Contents

List of Figures

List of Tables

Chapter 1

Introduction to Cosmology

1.1 General relativity

In 1915, Albert Einstein published one of the most monumental achievements in theoretical physics, reshaping our understanding of gravity and the very fabric of spacetime. This elegant and profound theory provides a comprehensive framework to describe the gravitational force, departing from the Newtonian paradigm that preceded it. Einstein's field equations serve as the mathematical foundation of General Relativity, expressing the intricate interplay between matter, energy, and the curvature of spacetime. The solutions to these equations have yielded groundbreaking predictions and have been verified through a myriad of experimental observations.

1.1.1 Equivalence principle

The equivalence principle in general relativity, or Einstein's equivalence principle, is one of the most important and revolutionary principles in physics, which allows us to understand the relationship between the mass of a body and the force of gravity. The first version of this principle, known as the *"weak equivalence principle"* was postulated by Galileo and Newton. This first aversion states that the inertial mass "m" and the gravitational mass "M" are equivalent [RV18]. These masses appear in the expressions for the force

$$\vec{f} = m\vec{a}, \tag{1.1}$$

$$\vec{f} = -M\nabla\phi. \tag{1.2}$$

with ϕ is the gravitational potential. However, some experiments have shown that there is no distinction between these masses, i.e. $m = M$. From these equations, notice that direct consequence is

$$\vec{a} = \ddot{\vec{x}} = -\nabla\phi(\vec{x}), \tag{1.3}$$

This indicates that the motion of particles in free fall is universal.

1.1.2 The metric

For a theory that can describe gravity in curved spaces, a general metric $g_{\mu\nu}$is necessary, which, in some limits, can reproduce the metric of a flat Minkowski space $\eta_{\mu\nu}$. Rather than conceptualizing gravity as an external force and describing particles navigating a gravitational field, we can integrate gravity into the metric. This idea allows us to discuss particles moving unhindered in a distorted or curved

space-time, where the metric cannot be uniformly transformed into Euclidean form throughout. In a four space-time dimensions the interval or the *invariant* for four-vectors (x_0, x_1, x_2, x_3) is

$$ds^2 = g_{\mu\nu} dx^\mu dx^\nu. \tag{1.4}$$

Where the Greek indices μ and ν range from 0 to 3, and we use the Einstein summation convention. Notice that the firts component is the time-like coordinate $(dx^0 = dt)$ and the last three are spatial coordinates. The metric $g_{\mu\nu}$ has four diagonal and six off-diagonal components, thus, is symmetric. In the special relativity case, the space is described by the Minkowski metric

$$\eta_{\mu\nu} = Diag(1, -1, -1, -1). \tag{1.5}$$

In the following sections we will know the metric that describes de expansion of the Universe.

1.1.3 Einstein Equations

The Einstein equation stands as a cornerstone of modern physics, embodying the profound insights of Albert Einstein into the nature of gravity and space-time. These equations were formulated in the early 20th century; the equation revolutionized our understanding of the Universe, reshaping the landscape of theoretical physics and cosmology. The journey towards the Einstein equation began with Einstein's revolutionary ideas on the nature of gravity. In 1905, Einstein presented his special theory of relativity, which fundamentally altered our understanding of space, time, and the constancy of the speed of light. Building upon this foundation, Einstein embarked on a quest to extend his theory to incorporate gravity [**Carrol_2019**].
The essence of general relativity lies in its ability to represent gravitation through a metric. However, another crucial aspect of general relativity connects this metric to the matter and energy present in the universe. This aspect is coded in the Einstein equations, which establish a relationship between the components of the Einstein tensor, describing the geometry, and the energy-momentum tensor, delineating the distribution of energy:

$$G_{\mu\nu} \equiv R_{\mu\nu} - \frac{1}{2} g_{\mu\nu} \mathcal{R} = 8\pi G T_{\mu\nu}. \tag{1.6}$$

In this equation, $G_{\mu\nu}$ is the Einstein tensor, $R_{\mu\nu}$ is the Ricci tensor given by

$$R_{\mu\nu} = \Gamma^\alpha_{\mu\nu,\alpha} - \Gamma^\alpha_{\mu\alpha,\nu} + \Gamma^\alpha_{\beta\alpha}\Gamma^\beta_{\mu\nu} - \Gamma^\alpha_{\beta\nu}\Gamma^\beta_{\mu\nu}, \tag{1.7}$$

with $\Gamma^\alpha_{\mu\nu}$ are the Christoffel symbols. Also, in the Einstein equations is present the Ricci scalar just given by $\mathcal{R} = g^{\mu\nu} R_{\mu\nu}$, and the energy-momentum for a perfect fluid is

$$T_{\mu\nu} = Diag(\rho, -p, -p, -p). \tag{1.8}$$

Notice that Einstein equation expresses the dynamic interplay between mass-energy and the geometry of space-time.

The importance of the Einstein equation extends beyond its mathematical elegance; it holds significant predictive power. As a framework, it enables the comprehension of various gravitational phenomena, encompassing planetary motion and the bending of light within gravitational fields. Particularly noteworthy is its prediction of gravitational waves, the ripples in the fabric of space-time. The detection of these waves in 2015 validated one of the final unconfirmed predictions of Einstein's theory and the presence of black holes in our universe, as confirmed by imaging the photon sphere of a supermassive black hole located at the center of the galaxy M87 in 2019.

The implications of the Einstein equation extend far beyond astrophysics and cosmology. It profoundly impacts understanding of the universe's origin, evolution, and ultimate fate. The equation plays a central role in cosmological models, such as the Big Bang theory, which seeks to elucidate the universe's history from its primordial beginnings to its present-day structure. Furthermore, the Einstein equation is the foundation for modern gravitational theories and has inspired generations of physicists to explore the frontiers of theoretical and experimental physics. From the enigmatic nature of black holes to the search for a unified theory of fundamental forces, the Einstein equation continues to fuel scientific inquiry and exploration.

In recent decades, cosmology has had an essential role in the scientific environment due to increasingly precise observations that allow us to know the universe in which we live in an increasingly detailed way. The observation that would start this revolution in contemporary cosmology, besides paralyzing the world of science, occurred in 1998 when Riess in the High-redshift Supernova Search Team and Perlmutter in the Supernova Cosmology Project Team independently reported the accelerated expansion of the universe by observing Type Ia supernovae (SN Ia).
Since this news, many proposals have emerged to explain this phenomenon. However, at present, using observational data, only two proposals can answer one of the most critical questions: *what causes the universe's accelerated expansion?* These proposals are known as Modified Gravity and *Dark Energy*.

1.2 Historical Context

The roots of cosmology stretch back to antiquity, where early civilizations crafted intricate cosmological narratives to explain the origin and nature of the universe. In Mesopotamia, the Babylonians envisioned a cosmos governed by divine order, with celestial bodies serving as omens and symbols of cosmic harmony. The Egyptians developed cosmological myths centered around the sun god Ra, whose journey across the sky represented the cycle of life, death, and rebirth.
In ancient Greece, philosophers such as Pythagoras, Plato, and Aristotle sought to understand the cosmos through reason and observation. Pythagoras proposed a mathematical harmony underlying the universe, while Plato envisioned a realm of ideal forms transcending the material world. Aristotle's cosmology posited a geocentric universe, with Earth at the center and celestial spheres rotating around it, setting the stage for centuries of cosmological thought rooted in anthropocentrism.

1.2.1 The Ptolemaic Universe

The Ptolemaic model, developed by Claudius Ptolemy in the 2nd century CE, represented the pinnacle of ancient cosmology. Based on Aristotle's teachings, Ptolemy's geocentric model depicted Earth as the stationary center of the universe, with celestial bodies orbiting around it in perfect circles. Epicycles and referents were introduced to account for the observed retrograde motion of planets, preserving the notion of celestial perfection within a geocentric framework.

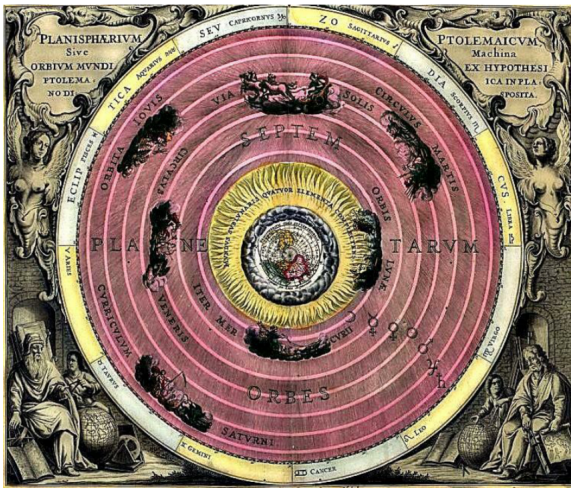

Figure 1.1: A Ptolemaic map of the world, created by Andreas Cellarius in 1708.

1.2.2 Copernican principle

The Copernican Principle is a fundamental pillar of contemporary cosmology, fundamentally altering humanity's understanding of the universe and our position within its vast expanse. Named after the Renaissance astronomer Nicolaus Copernicus, this principle embodies the revolutionary idea that Earth does not occupy a privileged position in the cosmos. Instead, it asserts that the laws of physics and the universe's properties are uniform and independent of any particular vantage point [Pee93].
The Copernican Revolution, initiated by Nicolaus Copernicus in the 16th century, marked a pivotal shift in humanity's cosmological worldview. Copernicus challenged the prevailing geocentric model, which posited Earth as the center of the universe, and proposed a heliocentric model where Earth and other planets orbited the Sun. This paradigm shift not only transformed our understanding of planetary motion but also laid the groundwork for the Copernican Principle, which asserts the absence of privileged positions in the universe. This principle can be summarized as follows

"On the Earth or in the Solar System, are not privileged observers of the universe"

The Copernican Principle guides modern cosmology, shaping our interpretation of observational data and theoretical frameworks. It forms the foundation of the cosmological principle, which asserts the universe's homogeneity and isotropy on grand scales devoid of favored positions or directions.
Observational astronomy provides compelling evidence in support of the Copernican Principle. Surveys of distant galaxies, cosmic microwave background radiation, and the large-scale distribution of matter all point to a vast, uniform

universe devoid of privileged locations. The cosmic microwave background, in particular, serves as a relic of the early universe, offering insights into its fundamental properties and evolution[Pla+20].

1.3 Cosmology

1.3.1 Isotropy and homogeneity

The vast expanse of galaxies, stars, and cosmic structures within the universe has perpetually captivated humanity with its intricate beauty and complexity. The fundamental concepts of isotropy and homogeneity are foundational in our comprehension of the universe's structure. These concepts, rooted in cosmology, provide crucial insights into the universe's large-scale properties and evolution over time. This essay explores the profound significance of isotropy and homogeneity, delving into their definitions, implications, and the evidence supporting their validity [Lid98] .

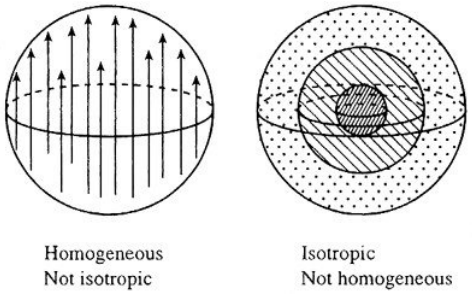

Figure 1.2: Homogenity and isotropy representation

The isotropy refers to the uniformity of the universe's properties in all directions. In an isotropic universe, observational data should not exhibit preferential directions or orientations; instead, they should appear statistically identical regardless of the observer's location or perspective.
The homogeneity denotes the uniform distribution of matter and energy throughout the universe on large scales. When observed on sufficiently large scales, a homogeneous universe exhibits a consistent density of cosmic structures, such as galaxies and galaxy clusters. This uniformity implies that the universe looks the same from any vantage point without distinct regions of higher or lower density.

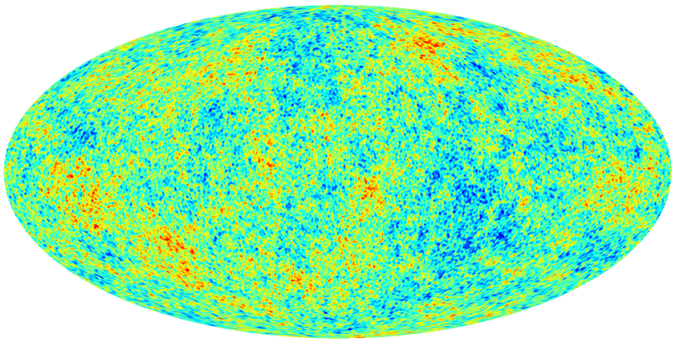

Figure 1.3: CMB map [Aur+21].

The homogeneity and isotropy in the Cosmic Microwave Background (CMB) provide compelling evidence for the cosmological principle. Observations of the CMB reveal a remarkably uniform temperature distribution across the sky, with temperature fluctuations at the level of one part in a hundred thousand. This uniformity suggests that the universe possesses a high degree of homogeneity on large scales, consistent with the predictions of the cosmological principle.

1.4 Friedmann-Robertson-Walker universe

The Friedmann-Robertson-Walker (FRW)metric is a solution to Einstein's field equations of general relativity and describes the geometry of a homogeneous, isotropic, and expanding universe. It encompasses three key components: homogeneity, isotropy, and cosmic expansion.
The FRW metric embodies the principles of the Cosmological Principle by providing a mathematical framework that describes a universe consistent with its assumptions. It allows cosmologists to model the universe's evolution and predict its properties based on observations. One of the remarkable implications of the FRW metric and the cosmological principle is the prediction of phenomena such as the redshift of distant galaxies and the CMB. Observations of the CMB, in particular, have provided compelling evidence for the isotropy and homogeneity of the universe, consistent with the predictions of the FRW metric and the Cosmological Principle.
The invariant element in this universe is

$$ds^2 = c^2dt^2 - a^2(t)\left(\frac{dr^2}{1-kr^2} + r^2\left(d\theta^2 + sin(\theta)d\phi^2\right)\right) \tag{1.9}$$

where $a(t)$ is the scale factor, and the constant k involves the following cases

- for $k = -1$, is a open universe.
- for $k = 0$, is a flat universe.
- for $k = 1$, is a closed universe.

The components of the Ricci tensor for this metric are

$$R_{00} = -\delta_{ii}\frac{\partial}{\partial t}\left(\frac{\dot{a}}{a}\right) - \left(\frac{\dot{a}}{a}\right)^2\delta_{ij}\delta_{ij} = -3\left(\frac{\ddot{a}}{a}\right). \tag{1.10}$$

$$R_{ij} = \delta_{ij}\left(2\dot{a}^2 + 2a\ddot{a}\right). \tag{1.11}$$

From this results we can to find the Ricci scalar

$$\mathcal{R} = -R_{00} + \frac{1}{a^2}R_{ii} = 6\left(\frac{\ddot{a}}{a} + \left(\frac{\dot{a}}{a}\right)^2\right) \tag{1.12}$$

From this elements, we can to calculate the components of the Einstein Equations, thus, the first component is

$$R_{00} - \frac{1}{2}g_{00}\mathcal{R} = 8\pi G T_{00}, \tag{1.13}$$

we get the first Friedmann equation

$$\left(\frac{\dot{a}}{a}\right)^2 = \frac{8\pi G}{3}\rho. \tag{1.14}$$

We need to define the ratio of the rate of change of the scale factor to the current value of the scale factor $a(t)$ or the *Hubble parameter* and the critical density

$$H(t) \equiv \frac{\dot{a}}{a}, \tag{1.15}$$

$$\rho_c \equiv \frac{3H_0^2}{8\pi G}. \tag{1.16}$$

Where H_0 is the present value of the Hubble parameter [PB22]

$$H_0 = 100\,h\,km\,sec^{-1}Mpc^{-1} = \frac{h_0}{0.98 \times 10^{10} years} = 74.2 \pm 3.6\,km\,sec^{-1}\,Mpc^{-1}, \tag{1.17}$$

and the value of the critical density at the present day is

$$\rho_{c0} = 1.88\,h_0^2\,\times 10^{-29} g\,cm^3. \tag{1.18}$$

The second Friedmann equation is obtained using the spatial components of the Einstein equations. This equations is

$$\frac{\ddot{a}}{a} = -\frac{4\pi G}{3}\left(\rho + 3P\right). \tag{1.19}$$

From these two equations, we can find the third equation deriving (1.14) with respect cosmic time and replacing (1.19). The last equation is the contuinity equation

$$\dot{\rho} - 3H\left(\rho + p\right) = 0. \tag{1.20}$$

In cosmology, the continuity equation is applied to various cosmic fluids to study their evolution over cosmic time. For example, it can describe the evolution of dark matter, baryonic matter (ordinary matter), and radiation in the expanding universe. By solving the continuity equation alongside other relevant equations, cosmologists can model the behavior of these cosmic fluids, predict their distributions, and understand their impact on the universe's large-scale structure.

1.5 Components of the universe

To understand the universe's evolution, it is necessary to know its components and dynamics. In cosmology, this entails defining the connection between mass density and pressure, known as the equation of state. Mathematically, this relation is $p = \omega\rho$, where ω is the equation of the state parameter (EoS). Currently, we will explore some potential scenarios [Lid98].

- **Matter:** In the Cosmology's context, the term *matter* is used for non-relativistic matter. This kind of the component is any material which has negligible pressure, i.e., $p = 0$.
  The case of a universe dominated by non-relativistic matter, from solving the continuity equation (1.20) we get

$$\rho_m = \rho_{m0} a^{-3}. \tag{1.21}$$

  The scale factor and the Hubble paramater in this case are

$$a(t) = \left(\frac{t}{t_0}\right)^{\frac{2}{3}}, \quad H(t) = \frac{2}{3t}, \tag{1.22}$$

  where t_0 is the present time.

- **Radiation:** For this case the pressure is $p = \rho c^3/3$, in the same way, solving (1.20) for an universe dominated by radiation, we can note

$$\rho_r = \rho_{r0} a^{-4}. \tag{1.23}$$

  The factor scale and the Hubble parameter are

$$a(t) = \left(\frac{t}{t_0}\right)^{\frac{1}{2}}, \quad H(t) = \frac{1}{2t}. \tag{1.24}$$

- **Curvature:** To keep the same notation in terms of the energy density, we can define the component associated with the curvature as follows

$$\rho_k \equiv -\frac{3k}{8\pi G a^2}. \tag{1.25}$$

  The EoS associated with the curvature is $\omega = -\frac{1}{3}$. Therefore, for an universe dominated by the curvature, the scale factor and the Hubble parameter are

$$a(t) = \frac{t}{t_0}, \quad H(t) = \frac{1}{t}. \tag{1.26}$$

- **Cosmological constant:** As we will see in the chapter (X) with more details, Einstein introduced the cosmological constant Λ to obtain a non-accelerated expansion universe . In the same way that the curvature case, is posible define de dark energy density for the cosmological constant

$$\rho_\Lambda = \frac{\Lambda}{8\pi G}. \tag{1.27}$$

  Furthermore, we can consider the cosmological constant associated with the vacuum energy, thus, this is the case of a perfect fluid with negative pressure, i.e., $\omega = -1$. Finally, for the case of an universe dominated by the cosmological constant, we get

$$a(t) \propto e^{\sqrt{\Lambda/3}t}, \;\; H(t) \text{ is a constant.} \tag{1.28}$$

It is convenient to define a new dimensionless density parameter for each componente of the universe. In the general form is given by

$$\Omega_i(t) \equiv \frac{\rho_i(t)}{\rho_c(t)}, \tag{1.29}$$

with ρ_c is the critical density previously defined. From this new definition, we can express the Friedmann constrain in the form

$$\Omega_\Lambda + \Omega_k + \Omega_m + \Omega_r = 1. \tag{1.30}$$

Another dimensionless quantity that is convenient to define in the context of cosmology is the *redshift* z, in the form

$$1 + z = \frac{a_0}{a(t_1)} \tag{1.31}$$

where a_0 is the scalar factor at the present time ($a_0 = 1$) and $a(t_1)$ is the scalar factor at an anarbitrary time t_1.
The Friedmann equation in terms of the dimensionless density parameters and the redshift is

$$H^2(z) = H_0^2 \left(\Omega_{k,0}(z+1)^2 + \Omega_{r,0}(z+1)^4 + \Omega_{m,0}(z+1)^3 + \Omega_{\Lambda,0}\right), \tag{1.32}$$

where $\Omega_{i,0}$ is the value of the dimensionless parameter at the present day for each component.

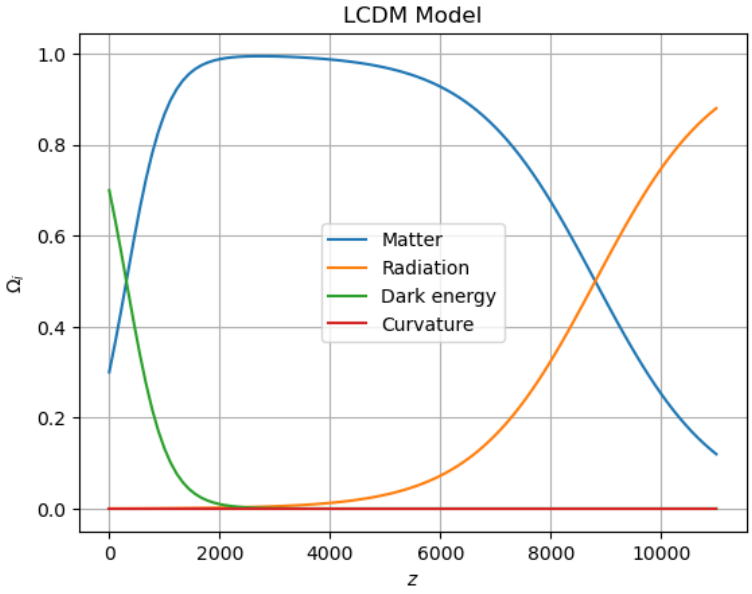

Figure 1.4: Evolution of the dimensionless density paramters.

Chapter 2

Dark Energy

In the early 20th century, Edwin Hubble reported one of the most important observations that would change our understanding of the cosmos. The Hooker telescope at Mount Wilson Observatory was used to measure the distance to Andromeda and other spiral nebulae; this showed that such nebulae are outside and far beyond the Milky Way. Shortly after that, by measuring the velocities of these galaxies and comparing them with their distances, he concluded that they were all moving away from each other. From these results, Hubble concluded that the universe was expanding. This chapter is about one of the proposals to explain this universe expansion, known as *dark energy*.

2.1 Observations

2.1.1 Cepheids

Because of their high luminosity compared to other stars, Cepheid variables are commonly used to calculate distances to objects beyond the Milky Way. These stars take their name from Delta Cephei, the first of this type discovered by John Goodricke in 1784, located in the constellation Cepheus.

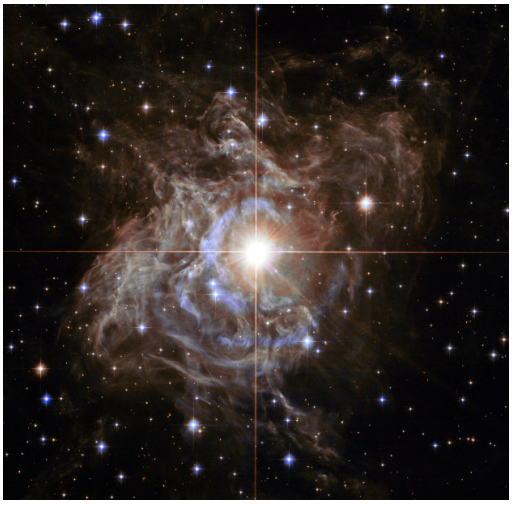

Figure 2.1: Image of the RS Puppis, the brightest Cepheid variable in the Milky Way [].

Cepheid variable stars are distinguished by their remarkable luminosity and brightness variations in a regular pattern. In 1912, astronomer Henrietta Leavitt made a crucial discovery while analyzing photographic plates: she observed that variable Cepheids in the Small Magellanic Cloud exhibited a relationship between their apparent brightness and the period of their luminous fluctuations. Although, at that time, the distance to the Magellanic Cloud was unknown, the Cepheids were assumed to be at approximately the same distance. Therefore, Leavitt established a systematic connection between the absolute luminosity of these stars and their period of oscillation: the brighter a Cepheid was, the longer its period of variation.
In 1923, Edwin Hubble and his team identified the presence of several Cepheid variable stars in the Andromeda Galaxy (M31). Using Henrietta Leavitt's calibration, Hubble could calculate the distance to M31 and thus prove that it was a separate galaxy. Until then, M31 was believed to be part of the Milky Way. After determining the distances to other galaxies using Cepheids, 1929, Edwin Hubble discovered that the speed at which a galaxy moves away from us is proportional to its distance

$$v = H_0 d, \tag{2.1}$$

this is the *Hubble's law* and tells us that the farther a galaxy is from us, the faster it moves away; this law can be interpreted as the result of the accelerating expansion of the Universe, which suggests the existence of an exotic form of energy called dark energy.

2.2 Supernovas

In 1998, two teams of researchers, the *High-redshift Supernova Search Team* (HSST) led by Riess and the *Supernova Cosmology Project* (SCP) led by Perlmutter, made observations that changed our understanding of the universe forever by discovering that the expansion of the universe is accelerating.
The benefit of utilizing type Ia supernovae for determining cosmological parameters lies in the simplicity of depicting the entire method within a single graph. The fundamental concept revolves around identifying an object with a well-established brightness, often called a "standard candle," and mapping it on a Hubble diagram. This diagram illustrates the relationship between brightness (magnitude) and redshift (z) [Per00].

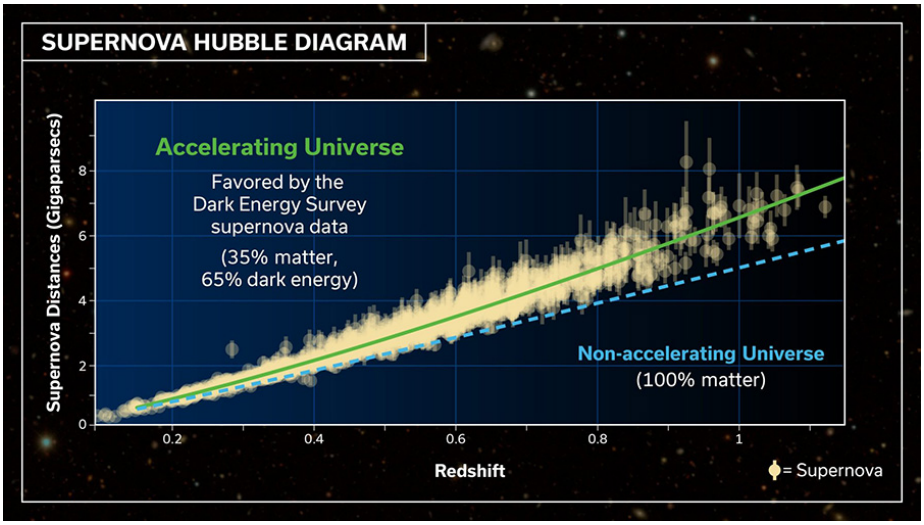

Figure 2.2: A history of size of the Universe **revisar esto**.

As we can see in the plot *citar* the confidence region for the 42 supernovae set, it becomes evident that the universe's expansion will continue indefinitely, and the universe is accelerating. However, these findings do not provide insights into the universe's curvature. The elongated confidence region spans across the line, representing a flat universe, distinguishing between closed and open curvature. Another significant inference drawn from the confidence region, is that the data significantly deviate from the most straightforward cosmological model, which assumes flatness and zero cosmological constant.

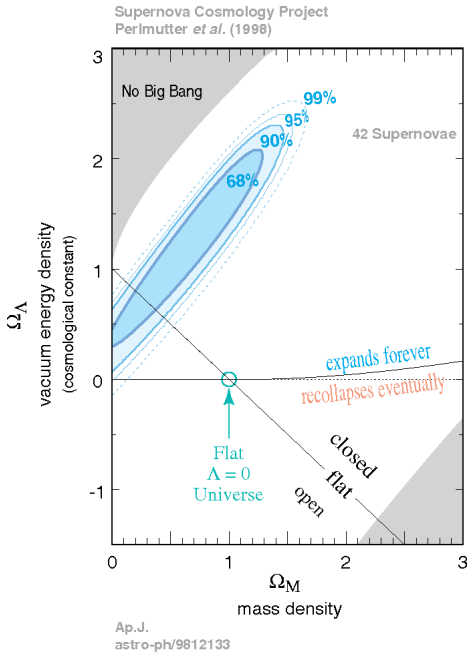

Figure 2.3: Plot for matter and vacuum density [Per00].

From these results, the universe's accelerated expansion is a fact; however, a new question, which to this day is one of the most important in cosmology, would arrive immediately: *what makes the universe expand in an accelerated way?* Again, one of the strongest candidates to explain this phenomenon is dark energy.

2.3 Cosmological Constant

In 1916, when Albert Einstein developed his general theory of relativity, the consensus of cosmology was that the universe was static, i.e., it did not expand. However, Einstein realized that his field equations describe a non-static universe. To reconcile his theory with this idea, introducing a new term into his equations was necessary to help counteract the effects of gravitational attraction. This new term introduced is known as the *cosmological constant* Λ.
The Einstein's equations (1.6) for this case are

$$R_{\mu\nu} - \frac{1}{2}\mathcal{R}g_{\mu\nu} + \Lambda g_{\mu\nu} = 8\pi G T_{\mu\nu}, \tag{2.2}$$

now the energy-momentum tensor takes the form

$$T_{\mu\nu} \longrightarrow T_{\mu\nu} - \frac{1}{8\pi G}\Lambda_{\mu\nu}. \tag{2.3}$$

The idea of the additional term associated with Λ comes from the fact that for an ideal fluid, which has an energy-momentum tensor given as

$$T_{\mu\nu} = (\rho_\Lambda + p_\Lambda)u_\mu u_\nu + p_\Lambda g_{\mu\nu}. \tag{2.4}$$

Because the introduction of the cosmological constant, the Friedmann's equations has a new term

$$H^2 = \frac{8\pi G}{3}\rho - \frac{k}{a^2} + \frac{\Lambda}{3}, \tag{2.5}$$

$$\frac{\ddot{a}}{a} = -\frac{4\pi G}{3}(\rho + 3p) + \frac{\Lambda}{3}.. \tag{2.6}$$

Notice that from these equation the importance of the cosmological constant. In the equation (2.6), for a cosmological constant $\Lambda > 0$, the contribution is positive, thus, it acts as a repulsive force. Furtheremore, for $\Lambda \ll 1$ the contribution of the constant is larger than the first term, leading to $\ddot{a}$, i.e., an accelerated expanding universe.
From the equation (2.4), we can consider the continuity equation for Λ

$$\dot{\rho} + \frac{3\dot{a}}{a}(\rho_\Lambda + p_\Lambda) = 0, \tag{2.7}$$

with ρ_Λ is a constant, notice that $\rho_\Lambda = -p_\Lambda$, thus, the cosmological constant can be consider as a fluid with negative effective pressure. This implies that as the Universe expands, the work is done on the cosmological constant fluid, which allows its energy density to remain constant despite the increase in the volume of the Universe.

2.3.1 Tensions in LCDM model

- **Fine-tuning problem**

  One of the main problems with the ΛCDM model occurs when we want the model to be consistent with the observations that confirm the universe's expansion. For this, we must be sure that the order of the cosmological constant is that of H_0^2, is say

$$\Lambda \approx H_0^2 = \left(2.133\, h \times 10^{-42}\, GeV\right)^2, \tag{2.8}$$

  with $h = 0.7$. Notice that we can consider an energy density associated, as follows

$$\rho_\Lambda \sim \frac{\Lambda}{8\pi}\, m_{pl}^2 \sim 10^{-47}\, GeV^4 \sim 10^{-123}\, m_{pl}^4, \tag{2.9}$$

  and where the Planck's mass is $m_{pl} \approx 10^{19}\, GeV$.
  To compare this value with the energy density of the zero-point ρ_{vacuum}, consider both as the energy associated with the vacuum. Recall that for an arbitrary field with momentum k, frequency, and mass m, the zero-point energy is

$$E = \frac{\left(k^2 + m^2\right)^{1/2}}{2}, \tag{2.10}$$

  for the total energy, we need to integrate over all zero-point energies, for a cut-off scale $k_{max} \ll m$, thus $\left(k^2 + m^2\right)^{1/2} \approx k$. The total vacuum enerdy density is

$$\rho_{vacuum} \approx \int_0^{k_{max}} \frac{4\pi k^3 dk}{2(2\pi)^3} = \frac{k_{max}^4}{16\pi^2}, \tag{2.11}$$

  and consider the cut-off scale k_{max} to be the Planck mass, because in General Relativity to be valid up to Plack scale, the vacuum energy density is

$$\rho_{vacuum} \approx 10^{74}\, GeV^4. \tag{2.12}$$

  From this, we can note the discrepancy between both energy densities is around 10^{121} times. This tension is know as the *fine-tuning problem.*

- **The coincidence problem**

  This other problem within the ΛCDM framework, is associated with the values of Ω_Λ and Ω_m, is almost the same in times very close to the present day. If we equal both density parameters and using the Friedmann's constrain at the present time for an Universe dominated by matter and vacuum, it is possible to find the redshift assiated

$$z_{equality} = \left(\frac{\Omega_{\Lambda 0}}{1-\Omega_{\Lambda 0}}\right)^{1/3} - 1 \approx 0.3, \tag{2.13}$$

  for the vacuum's density parameter at the present time $\Omega_{\Lambda,0} \approx 0.7$.

  More specifically, during the universe's expansion, the density of matter decreases with time due to dilution caused by the increase in volume. In contrast, the density of dark energy remains relatively constant or even increases. This means that matter density was dominant over dark energy in earlier epochs. Still, in the present epoch, both densities are of the same order of magnitude, giving rise to why this is happening just now in cosmic history.
  The coincidence problem raises questions about whether this situation is a chance occurrence or whether there is some underlying principle or physical mechanism explaining why these densities are comparable in the present epoch. Resolving this problem could offer a deeper understanding of the nature of dark energy and its relationship to the universe's evolution.

2.4 Beyond LCDM model

Chapter 3

Holographic dark energy models

3.1 Black holes and holographic principle

Black holes are enigmatic celestial objects that have captivated the imaginations of scientists and the general public alike. These mysterious entities are characterized by their extreme gravitational forces, so intense that not even light can escape their grasp. The concept of black holes emerged from Albert Einstein's theory of general relativity, which predicted the possibility of such collapsed objects with gravitational fields so strong that they create a region from which nothing, not even electromagnetic radiation, can escape. The term *"black hole"* was coined by physicist John Archibald Wheeler in 1967, solidifying the idea of these cosmic anomalies.
The study of black holes has witnessed significant advancements, with observations providing crucial insights into their properties. Notable achievements include the detection of gravitational waves resulting from the merger of black hole pairs, as observed by the Laser Interferometer Gravitational-Wave Observatory (LIGO) and Virgo collaborations. Additionally, the Event Horizon Telescope (EHT) made history by capturing the first-ever image of a black hole's shadow in the center of the galaxy M87.
Understanding black holes plays a pivotal role in unraveling the mysteries of the universe, including the nature of space-time and the behavior of matter under extreme conditions. While much progress has been made, numerous questions surrounding black holes, such as the nature of their singularities and the connection between gravity and quantum mechanics, continue to challenge our understanding of the cosmos.

3.1.1 The Schwarzschild Black Hole

In General Relativity the metric for the Schwarzschild black hole is

$$ds^2 = \left(1 - \frac{2MG}{r}\right) dt^2 - \left(1 - \frac{2MG}{r}\right)^{-1} dr^2 - r^2 d\Omega^2, \tag{3.1}$$

where M is the black hole mass, G the gravitational constant and $d\Omega^2$ the volume element of the 2-sphere.
For this blanck hole, there are two singularities in this metric, at $r = 0$ (gravitational singularity) and the at the Schwarzschild radius $r = 2MG$, the last one defines the all important horizon. Note that the horizon is not a mathematical singularity of the black hole geometry. To better understand this distinction, consider a small angular region associated with a point on the

horizon. Now we need to define a new variable in the following form

$$y = r - 2MG, \tag{3.2}$$

and for the case $y \ll 2MG$ the metric has the form

$$ds = \frac{y}{2MG}dt^2 - \frac{2MG}{y}dy^2 - dx^i dx^i. \tag{3.3}$$

To rewrite the above expression in a simpler version, consider

$$\rho = \sqrt{8MGy}, \tag{3.4}$$

$$\omega = \frac{t}{4MG}. \tag{3.5}$$

Using the new variables, the metric has the form

$$ds^2 = \rho^2 d\omega^2 - d\rho^2 - dx^i dx^i. \tag{3.6}$$

Observe that this equation is the typical metric of the Minkowski space in hyperbolic polar coordinates. To finding the maximal analytic extension of the Schwarzschild metric, i.e. a coordinate system in which all geodesics that do not terminate on a physical singularity can be extended to arbitrary values of their affine parameters. For this case, it is given by the *Kruskal-Szekers* coordinates

$$V = \rho e^{\omega}, \tag{3.7}$$

$$U = -\rho e^{-\omega}. \tag{3.8}$$

The expression (3.6) takes the form

$$ds^2 = \frac{32G^3M^3}{r}e^{-\frac{r}{2GM}}dUdV - dx^i dx^i. \tag{3.9}$$

Sometimes another set of coordinates is used given by

$$T = \frac{1}{2}(U+V) = \left(\frac{r}{2MG} - 1\right)^{1/2} e^{\frac{r}{4MG}} sinh\left(\frac{t}{4MG}\right) \tag{3.10}$$

$$R = \frac{1}{2}(V-U) = \left(\frac{r}{2MG} - 1\right)^{1/2} e^{\frac{r}{4MG}} cosh\left(\frac{t}{4MG}\right) \tag{3.11}$$

Observe that $T^2 - R^2 = \left(1 - \frac{r}{2MG}\right)e^{r/2MG}$, in these coordinates, the radial null curves are simpply $T = \pm R + constant$, as in Minkowski. Surfaces with $r = constant$, correspond to $T^2 - R^2 = constant$ (hyperbolae) and surfaces with constant t are $T/R = tanh\left(\frac{t}{4MG}\right)$.
The maximal extension is valid for any (T, R) that do not hit the singularity at $r = 0$, and correspond to $T^2 - R^2 < 1$ with $-\infty \leq R \leq \infty$. It is an analytical extension valid beyond $r < 2GM$ where the definition suggets that it becomes imaginary, This defines the Krusal diagram.
From the diagram (X), the following cases are identified

- For $r > 2GM$, the region covered by our original coordinates.

- The region II is the black hole, all future-directed paths hit the singularity.

- The region III, is the *"white hole "*.

- The region IV, is disconeected from the us and it is another asymptotically flat region of spcacetime. At $R = T = 0$, I and II are connected by a *"wormhole"*.

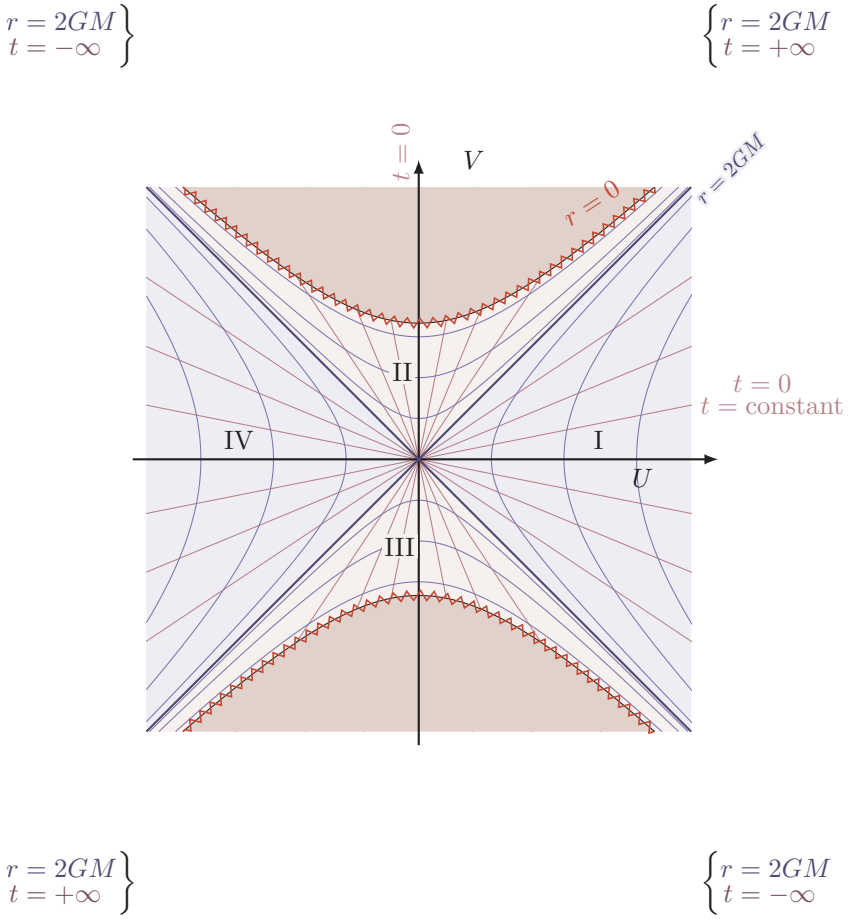
$r = 2GM$
$t = -\infty$
$r = 2GM$
$t = +\infty$
$t = 0$
V
$r = 0$
$r = 2GM$
II
$t = 0$
$t = \text{constant}$
IV
I
U
III
$r = 2GM$
$t = +\infty$
$r = 2GM$
$t = -\infty$

3.2 Black Hole Thermodynamics

To better understand the nature of black holes, it is necessary to consider other intrinsic aspects of these incredible objects, such as their thermodynamics. Thus, in addition to considering the previously mentioned characteristics of a black hole system, such as its mass, we must consider its entropy and temperature. To make the thermodynamic description of a Black Hole it is necessary to use quantum field theory, as we will see below.
In special relativity, the usual time for Minkowski space-time is given by

$$x^0 = \frac{U+V}{2}, \tag{3.12}$$

with conjugate to it is the momentum component p_0. Note that, the this component is not the associated energy or Hamiltonian appropriate to the study of black hole by distant observers, since the natural time of these observers is the Schwarzchild time

$$t = 4MG. \tag{3.13}$$

For black holes, the conjugate Hamiltonian which represents its energy or mass is

$$H_t = \frac{1}{4MG} H_\omega \tag{3.14}$$

with H_ω is the dimensionless Hamiltonian conjugate to the dimensionless Rindler time ω.
Now consider an observer outside the horizon has no the degrees of behind the horizon, thus all observations can be described in terms of a density matrix $\mathcal{R}$, obtained by tracing over the degrees of freedom behind the horizon. Is necesary derivate the form of the density matrix for an external observer, for this, we begin with the Minkowski space-time vacuum using the coordinates of Minkowski spcace given by

$$x^0 = \frac{V+U}{2}, \tag{3.15}$$

$$x^3 = \frac{V-U}{2}, \tag{3.16}$$

and the horizon coordinates x^i. Note that for the case for the instant of Rindler time $\omega = 0$, we can see that coincides with the half-surface

$$x^0 = 0, \tag{3.17}$$

$$x^3 > 0. \tag{3.18}$$

The region for $x^3 < 0$ (the other half of the surface) is behind the horizon and is to be traced over.

For a description from the quantum field theory, consider a set of quantum fields ϕ and observe that to specify the field configuration at $x^0 = 0$, is necessary to give the values of ϕ on both half-surfaces, for this, consider ϕ_a as the field configuration for $x^3 > 0$ and ϕ_b for $x^3 < 0$. For this system, the quauntum state is represented by the following wave function

$$\Psi(\phi) = \Psi(\phi_a, \phi_b). \tag{3.19}$$

To find the form of Ψ, we use the standard Euclidean Feynman path integral formula

$$\Psi(\phi_a, \phi_b) = \int d\phi e^{-S}, \tag{3.20}$$

here the path integral is over all fields for the region $ix^0 > 0$ with the boundary condition is $\Psi(\phi_a, \phi_b)$ at $x^0 = 0$. To compute $\mathcal{R}$, we consider divide the upper half plane ix^0 in to infinitesimal angular wedges, thus, the path integral can then be evaluated in terms of a generator of angular rotations. For the Minkowski vacuum, the wave functional can be expressed by

$$\Psi(\phi_b, \phi_a) = \langle \phi_b | \exp(-H_\omega \pi) | \phi_a \rangle. \tag{3.21}$$

The general form of the density matrix is

$$\mathcal{R} = \int \Psi^* (\phi_b, \phi'_a) \Psi (\phi_b, \phi_a) \, d\phi_b. \tag{3.22}$$

Using the equation (3.21) and the above equation, we find

$$\mathcal{R} = \langle \phi'_a | \exp(-2\pi H_\omega) | \phi_a \rangle = \exp\left(-\frac{H_\omega}{T_\omega}\right), \tag{3.23}$$

where $T_\omega = \frac{1}{2\pi}$. Notice that the expression (3.23) is a thermal density matrix for temperature T_ω, furthermore, the previous derivatios is exact and no way replies on the free field approximation, therefore, is valid for any quantum field theory for any strength of coupling. [1]
Using the equation (3.6) to convert to a proper temperature with the correct dimensions of energy, consider the interval $ds = \rho d\omega$. The proper temperature for an observer at distance ρ from the horizon is

$$T(\rho) = \frac{T_\omega}{\rho} = \frac{1}{2\pi\rho}. \tag{3.24}$$

Notice that the expression (3.24) is an important result; for an observer outside a black hole (but in the near horizon region), the temperature varies as the inverse distance from the horizon for the observer.

[1] Due the Rindler Hamiltonian and the Rindler time are dimensionless, the temperature T_ω does not have the usual dimensions of energy.

Now consider a distant observer asymptotically far from the black hole, which measures the temperature, for this case the proper time is the Schwarzschild time $t = 4MG\omega$. The temperature measured by the observer is

$$T_H = \frac{T_\omega}{4\pi MG}. \quad \text{Hawking temperature} \tag{3.25}$$

This is the true thermodynamic temperature of an isolated black hole.

3.2.1 Black Hole Entropy

To find the thermodynamic relation between the mass (energy) and the temperature is necessary to compute the associated entropy with the black hole, for this, consider the equation of state

$$dM = TdS, \tag{3.26}$$

integrating this expression, we find in terms of the horizon area A

$$S = \frac{A}{4G}. \quad \text{Bekenstein-Hawking formula} \tag{3.27}$$

This expression for the entropy applies to every kind of black hole, be it rotating, charged or in arbitrary dimensions. For the general case in $(d+1)$ dimensions, the concept of two dimensional area only needs to be replaced by the $(d-1)$ dimensional measure of the horizon which we continue call area.
In order to establish the idea of the holographic principle, consider a large region of the space Ω and for simplicity, this region is a sphere. Now consider the space of states that describe arbitrary systems that can fit into Ω such that the region outside ω is empty space.
Consider that we are dealing with a lattice of spins, in this way, the lattice spacing is l, the volume of the region is V_Ω , the number of spins is V/a^3 and the number of orthogonal states in Ω is

$$N_{states} = 2^{\frac{V_\Omega}{l^2}} \tag{3.28}$$

In the analysis of a system's states, entropy assumes a pivotal role. Generally, entropy is not merely an intrinsic property of a specific system but is also intertwined with one's knowledge about the system. To characterize entropy, we initiate the definition with certain constraints that articulate our understanding of the system, such as the energy within specified limits, angular momentum, and any other pertinent information available.
Entropy is formally defined as the logarithm of the number of quantum states adhering to the specified constraints. Thus, the maximum entropy is the logarithm of the total number of states, i.e., the entropy, given that we know

nothing about the state of the system. The maximum entropy for the spin system is

$$S_{max} = \frac{Vlog(2)}{l^3}. \tag{3.29}$$

Notice that the maximum entropy is directly proportional to the system's volume. To be more precise, it is proportionate to the quantity of essential degrees of freedom required to depict the system.

System with gravity.

Let's contemplate a system incorporating gravitational effects. Once more, we concentrate on a spherical space region denoted as Ω encompassed by a boundary labeled $\partial\Omega$ and with an area A. Imagine a thermodynamic system characterized by entropy S entirely confined within the space defined by Ω. It is essential to note that the aggregate mass of this system must not surpass the mass corresponding to a black hole with an area of A as exceeding this limit would result in a size larger than the defined region.
Now, envision the collapse of a spherically symmetric shell of matter with precisely the right amount of energy so that it forms a black hole that fills the region together with the original mass. In simpler terms, the area of the black hole's horizon is denoted as A. The outcome of this process yields a system with a known entropy, represented as S. Utilizing the second law of thermodynamics, we can deduce that the initial entropy within the region denoted as Ω must have been less than or equal to $S = A/4G$. This condition implies that the maximum entropy of a spatial region is directly proportional to its area, measured in Planck units. Such limitations are commonly referred to as *holographic bounds*.

3.3 Standard holographic dark energy model

The first model of holographic dark energy is based on the Bernstein-Hawking formula (3.27) and the limits if the vacuum energy density from the quauntum field theory developed by Cohen, Kaplan y Nelson in 1999 [**articleCohen**].
In high energy physics, the description of the systems uses an effective field theory (EFT) with a certain ultraviolet (UV) cutoff, which must be smaller than the Planck mass M_p, as long as all moments and field strengths are always small compared to the cutoff. However, even though these effective theories have had great success in high-energy physics, their application to other systems is not always possible; for example, the Nature of systems such as black holes suggests that the underlying theory of Nature cannot be a local quantum field theory. To solve this problem, it is necessary to establish a relationship between the UV and infrared (IR) limits.
Consider an efective quantum field theory for a region, for example, a box of dimension L and with the ultreaviolet cutoff Λ, the entropy assiated at this region is around $S \sim L^3\Lambda^3$. Notice that from the Bekenstein results, the maximun entropy in a box of volume L^3, is only proportional to the area of the box, from that, for a some cutoff Λ. always there is a finite large volume with an entropy of an EFT will not exceed the Bekenstein limit. From the Bekenstein-Hawking and we can establish the above as

$$L^3\Lambda^3 \lesssim S_{BH} \sim L^2 M_p^2, \tag{3.30}$$

where consider L as the radius of the black hole. Now, from the maximum energy density in EFT $\sim \Lambda^4$, the constrain takes the form

$$L^3\Lambda^4 \lesssim L M_p^2, \tag{3.31}$$

This can be expressed

$$\rho_{de} L^4 \lesssim S, \tag{3.32}$$

where S is an arbitrary entropy and $S \propto A \propto L^2$ and the Planck mass is given as $M_P^{-2} = 8\pi G$. For the largest allowed value of L, the equality is satisfied as follows

$$\rho_\Lambda = 3c^2 M_p^2 L^{-2}. \tag{3.33}$$

As we saw earlier, it is possible to describe the entropy of a black hole in a well-defined way. However, as usual in physics, it is often necessary to add new parameters to the already known quantities to make a more complete system description. This is why many entropy models have been proposed to describe systems like black holes better and, as expected, always in some limit, reproduce the already known Bekenstein-Hawking formula. The properties that we expect generalized versions of the entropies to have are [NF22]

- **Bekenstein-Hawking limit:**
  All the above entropies reduce to the Bekenstein-Hawking entropy S_{BH} in an appropriate limit.
- **Monotonically increasing functions:**
  All the above entropies are monotonically increasing functions of the S_{BH}.
- **Positivity:**
  All the above entropies are positive, as is the Bekenstein-Hawking entropy.
- **Generalized third law:**
  In the third law of standard thermodynamics for closed systems in thermodynamic equilibrium, the quantity $e^{S_{BH}}$ expresses the number of states, or the volume of these states, and therefore the entropy vanishes when the temperature does because the ground (vacuum) state should be unique. By contrast, the Bekenstein-Hawking entropy diverges when the temperature T vanishes and it goes to zero at infinite temperature. However, requiring any generalized entropy to vanish when the Bekenstein-Hawking entropy vanishes could be a natural requirement.

As we will see, the following generalized entropy alternatives share these characteristics.

3.4 Barrow holographic dark energy model

This model arose from the ideas of John D. Barrow in 2020 when he was interested in knowing the consequences for the black hole area of introducing a fractal structure for the horizon geometry.
Barrows proposed to model the horizon surface of a black hole as a fractal horizon surface. This fractal is constructed by joining several small spheres so that they touch their outer surface, with even smaller spheres touching the surfaces of those spheres, and so on consecutively. In this way, the most general case is when the surface of the black hole is only the fractal surface, the surface are vary as $R^{2+\mathcal{B}}$ with the constrain $0 \leq \mathcal{B} \leq 1$. Notice the case when $\mathcal{B} = 0$, is the simplest horizon structure and the case $\mathcal{B} = 1$ is associated from an information perspective as if it possessed one geometric dimension higher. From this, the black hole entropy vary as [Bar20]

$$S \approx \frac{A}{A_{pl}} \sim \frac{A_g}{A_{pl}}^{1+\frac{\mathcal{B}}{2}}, \tag{3.34}$$

where $A_g \approx (ct_0)^2$, with the cosmic time at the present $t_0 \sim 10^{17}\, s$ and A_{pl} the Planck's mass. For this reason, Barro's entropy is usually expressed as

$$S = \left(\frac{A}{A_p}\right)^{1+\mathcal{B}/2} \tag{3.35}$$

From the above definition of entropy, as in the case of the Bekenstein-Hawking entropy, it is possible to find expressions for the dark energy density using the equation (3.33), we get for the case of the Barrow entropy

$$\rho_B = 3c^2 M_p^2 L^{2-\mathcal{B}} \tag{3.36}$$

3.5 Tsallis holographic dark energy model

Tsallis entropy, named after Constantino Tsallis, who introduced it in the 1980s, is a generalization of the classical Boltzmann-Gibbs entropy commonly used in statistical mechanics. Unlike the Boltzmann-Gibbs entropy, which is based on the logarithmic function, Tsallis entropy is based on a $q-logarithmic$ function, where $q \in \mathbb{R}$ is a parameter that characterizes the deviation from the classical case [Tsa88].

Usin the multifractal concepts and the probability p_i^q associated to an event, Tsallis postulated its entropy for the purpose of generalize the standard expression of the entropy S in the information theory

$$S = -k \sum_{i=1}^{W} p_i ln(p_i), \ \forall \ W \in \mathbb{N}. \tag{3.37}$$

where W represents the total number of possibl configurations. The generalized version by Tsallis is

$$S_q = k \frac{1 - \sum_{i=1}^{W} p_i^q}{q-1}, \tag{3.38}$$

with k a conventional and $\sum_{i=0}^{W} p_i = 1$.
In 1902, Gibbs highlighted a limitation of the Boltzmann-Gibbs theory, noting its inapplicability to systems with divergent partition functions. We now understand that gravitational systems fall into this category. Tsallis later demonstrated that in such instances, the conventional Boltzmann-Gibbs additive entropy, grounded in the assumption of weak probabilistic correlations and their association with ergodicity, requires generalization. This leads to the concept of non-additive entropy, where the entropy of the entire system may not necessarily equal the sum of the entropies of its subsystems, this is the case of the Tsallis entropy [Sar+18]. For the case of a hole, the Tsallis entropy can be expressed as

$$S_T = \frac{A_0}{4G} \left(\frac{A}{A_0} \right)^{\mathcal{T}}, \tag{3.39}$$

with A_0 is area constant and $\mathcal{T}$ is a dimensionless parameter. Notice that for $\mathcal{T} = 1$ the Bekenstein-Hawking is recovered.
From the above definitions of entropy, as in the case of the Bekenstein-Hawking entropy, it is possible to find expressions for the dark energy density using the equation (3.33), we get for the case of the Tsallis entropy

$$\rho_T = AL^{2\tau - 4}. \tag{3.40}$$

3.6 Kaniadakis holographic dark energy model

Kaniadakis entropy is a concept that arises in the context of information theory and statistical mechanics and is related to the generalized entropy theory proposed by Constantine Tsallis. While Shannon entropy is a standard measure of uncertainty in a system, Tsallis entropy generalizes this concept to include non-extensive systems and systems exhibiting long memory phenomena.
Giorgio Kaniadakis further extended Tsallis' idea of generalized entropy. Kaniadakis's entropy is defined similarly to Tsallis's entropy but with a different functional expression. Instead of the exponential form use d by Tsallis, the Kaniadakis function uses a Levy distribution form. This distribution function is a generalization of the Gaussian distribution. It has the property of having heavier tails, which makes it suitable for describing systems with high nonlinearity and long-term correlation characteristics [KS23]. This entropy is

$$S_k = -k_B \sum_{i=1}^{W} \frac{\left(P_i^{1+K} - P_i^{1-K}\right)}{2K} \tag{3.41}$$

with K_B is the Boltzmann's constant and W is the total number of the system configurations. For our purposes is convenient consider $k_B = c = \hbar = 1$.
As the case of the Tsallis entrpy, is posible to applied the Kaniadakis entropy to black holes thermodynamics. The way for this is by assuming $P_i = 1/W$ and using the Boltzamnn-Gibbs entropy, from this, we establish the the probability relation to the Bekenstein-Hawking entropy as

$$P_i = e^{-S_{BH}}, \tag{3.42}$$

and find the usual expression for the Kaniadakis entropy, that is

$$S_K = \frac{sinh(KB_{BH})}{K}, \tag{3.43}$$

where K is the Kaniadakis parameter. Notice the case when $K \to 0$, the Bekenstein-Hawking entropy is recovered. Furtheremore, notice that when the deviation from the standard entropy in small, we can approximate the Kaniadakis entropy as

$$S_K \approx S_{BH} + \frac{K^2}{6} S_{BH}^3, \tag{3.44}$$

the second term can be consider as a correction term to the black hole entropy. From this expansion of the Kaniadakis entropy, the dark energy density for the Kaniadakis holographic dark energy (KHDE) is

$$\rho_K = 3c^2 M_p^2 L^{-2} + K^2 M_p^6 L^2 \tag{3.45}$$

3.7 posible propuesta

The entropy models can be summarized in the following table

Model	S
Bekenstein-Hawking	$\frac{A}{4G}\cdot$
Barrow	$\left(\frac{A}{A_p}\right)^{1+\mathcal{B}/2}$
Tsallis	$\frac{A_0}{4G}\left(\frac{A}{A_0}\right)^{\mathcal{T}}$
Kaniadakis	$\frac{sinh(KB_{BH})}{K}$
Propuesta	x

3.7.1 FUTURE EVENT HORIZON AS THE CHARACTERISTIC LENGTH SCALE

If the maximum allowed value of L, can be taken as the current size, i.e., at the Hubble scale ($L = H^{-1}$), it is possible to consider this energy density as the one associated with dark energy at present. If one considers a Universe that is dominated only by vacuum and matter, the associated Friedmann equation in Planck units can be expressed, as expresses

$$\rho = 3M_p^2 H^2. \tag{3.46}$$

Hsu showed in 2004 that this choice on the scale of L is incorrect [Hsu04] because the resulting equation of state for dark energy is $\omega = 0$. Based on this result, Hsu points out there is the possibility that entropy bounds may only apply to Λ on a cosmological scale. Thus, there is no apparent reason why the concept of holography couldn't be extended to smaller systems within our universe.
To solve the problem that Hsu had discovered and obtain an expanding universe, Miao Li, in 2004, proposed a new horizon by a shrinking Hubble scale [Li04]. This horizon is called the future event horizon, defined as

$$R_h = \int_t^\infty \frac{dt}{a} = \int_a^\infty \frac{da}{Ha^2}. \tag{3.47}$$

Now by definition $R^2\Omega_{de}H^2 = c^2$ or [Li04]

$$R_h = \frac{L}{a} = \frac{c}{Ha\sqrt{\Omega_{de}}}. \tag{3.48}$$

Taking the derivate to find an expression for $\dot{H}$, we get

$$\frac{\dot{H}}{H} = \frac{H\sqrt{\Omega_{de}}}{c} - H - \frac{\dot{\Omega}_{de}}{2\Omega_{de}} \tag{3.49}$$

Taking $L = R_h$ in the other definitions of dark energy density for each model and solving for the horizon, we find equivalent expressions in each case

$$\int_x^\infty \frac{dx}{Ha} = \frac{1}{a}\left(\frac{A}{3M_p^2H^2\Omega_{de}}\right)^{\frac{1}{4-2\tau}}, \text{ Tsallis model.} \tag{3.50}$$

$$\int_x^\infty \frac{dx}{Ha} = \frac{1}{a}\left(\frac{c^2}{H^2\Omega_{de}}\right)^{\frac{1}{2-B}}, \text{ Barrow model.} \tag{3.51}$$

Chapter 4

Bayesian statistics

Bayesian statistics is an approach that relies on the Bayesian interpretation of probability, where probability is conceived as a measure of uncertainty or degree of belief regarding the occurrence of an event. Unlike frequentist statistics, which focuses on the relative frequency of long-term events, Bayesian statistics integrates prior information (called a priori information) with observed evidence to update beliefs and make inferences about model parameters or predictions.

4.1 Theorem of Bayes

For two events 'A' and 'B', the theorem of Bayes establishes the relation

$$P(B|A) = \frac{P(A|B)P(B)}{P(A)} \tag{4.1}$$

where $P(A|B)$ is the probability of event A occurring given that event B has occurred, known as *the posterior probability.* $P(B|A)$ is the probability of the event B ocurring given that event A has occurred, it is know as *likelihood.* $P(A)$ is the a priori probability of event A i.e., the probability that A occurs before B is observed and the analogous form for $P(B)$.
In the Bayesian framework, the data and the model are un the same space. For this reason, for a given model H (hypothesis) we consider D as A, i.e., a set of data. In the same way, we consider θ as Bm i.e. the parameter vector of said hypotesis. The theorem of Bayes takes the form

$$P(\theta|D,H) = \frac{P(D|\theta,H)P(\theta|H)}{P(D|H)} \,. \tag{4.2}$$

where

- Is usually express the likelihood as $L(D|\theta,H) = P(D|\theta,H)$.
- The prior as $\pi(\theta) = P(\theta|H)$, is the knowledge about the model.
- And $\mathcal{Z} = P(D|H)$ is the evidence of the model, usually know as *Bayesian Evidence.*

The Bayesian Evidence can be calculated from the formula

$$\mathcal{Z} = \int d^N\theta P(D|\theta,H)P(\theta|H). \tag{4.3}$$

In this espression we consider a parameter space with dimension N. The Bayesian evidence is crucial in determining the model that most accurately represents the data, a process commonly referred to as model selection. For this reason, is useful to define the ratio of the two evidence

$$K \equiv \frac{P(D|H_1)}{P(D|H_2)} = \frac{\mathcal{Z}_1}{\mathcal{Z}_2}. \tag{4.4}$$

From this definition, we can define another quantity known as *Bayes factor*

$$\mathcal{B}_{1,2} = ln(K) = ln(\mathcal{Z}_1/\mathcal{Z}_2), \tag{4.5}$$

This factor provides an insight into the extent to which Model 1 might adequately explain the data in comparison to Model 2, for example.
The significance of Bayes' theorem in statistical inference is immense. In conventional practice, we often gather data and interpret it using a predefined model. However, the inverse is often true: we initially possess a dataset and then assess various models' suitability based on the probability of fitting the data. Bayes' theorem offers a mechanism to bridge these two approaches. By leveraging Bayes' theorem, we can effectively determine the model that most accurately aligns with the observed data.
For a better interpretation of the Bayes factor, the *Jeffreys guideline scale* is used to measure the comparative evidence supporting one model over another. This criterion can be summarized as follows

Jeffreys guideline scale			
$\lvert\mathcal{B}_{1,2}\rvert$	Odds	Probability	Strength
> 5.0	$> 150:1$	> 0.993	Decisive

4.2 Likelihood and Chi-squeare

4.3 Confidence regions

4.4 Markov Chain Monte Carlo

Chapter 5

Results

5.1 Differential equation for each model

To find a general expression for the evolution of the holographic dark energy, consider the derivate respect to cosmic time of the dark energy density parameter, and using its respective conservation equation. We get the general differential equation

$$\dot{\Omega}_{de} = -3H(1+\omega_{de})\Omega_{de} - 2\Omega_{de}\frac{\dot{H}}{H}, \tag{5.1}$$

We need to replace ω_{de} in terms of the density energy and pressure and using the Friedmann constrain, the differential equation takes the form

$$\dot{\Omega}_{de} = 2\frac{\dot{H}}{H}(1-\Omega_{de}) + 3H\left(1-\Omega_{de}+\omega_l\Omega_l\right), \tag{5.2}$$

where the index l refers to other cosmological quantities. Now note that in this general equation, we can use each holographic model sustituying the expression of the $\dot{H}$ which is obtained in each model.
For the first and the most simple case, the standard holographc dark energy, this value is given by (3.49) and the associated differential equation is

$$\frac{1}{\Omega_{de}}\frac{d\Omega_{de}}{dz} = \frac{\Omega_{de}-1}{z+1}\left(1+\frac{2\sqrt{\Omega_{de}}}{c}\right) - \frac{3\Omega_l\omega_l}{z+1} \tag{5.3}$$

where we introduce the new variable $x = ln(a)$ and the derivate with respect to this variable.
For the case of the Barrow Holographic dark energy model the evolution of the Hubble parameter is

$$\frac{\dot{H}}{H^2} = -\frac{3}{2-\mathcal{B}}\left(1+\omega_{de}\Omega_{de}\right), \tag{5.4}$$

we have the following differential equation in the framework BHDE

$$\Omega'_{de} = \Omega_{de}\left(1-\Omega_{de}\right)\left(1+\mathcal{B}+(2-\mathcal{B})\left(\frac{\Omega_{de}}{c^2}\right)^{\frac{1}{2\mathcal{B}}}\right), \text{ Barrow} \tag{5.5}$$

We can do the same procedure for the other two remaining models and find the following differential equations

$$\Omega'_{de} = \Omega_{de}\left(1-\Omega\right)\left(2\delta - 1 + Q\left(1-\Omega_{de}\right)^{\frac{1-\delta}{2(2-\delta)}}\left(\Omega_{de}\right)^{\frac{1}{2(2-\delta)}} e^{\frac{3(1-\delta)}{2(2-\delta)}x}\right), \text{ Tsallis model} \tag{5.6}$$

where

$$Q = 2(2-\delta)\left(\frac{B}{3M_p^2}\right)^{\frac{1}{2(\delta-2)}}\left(H_0\sqrt{\Omega_{m0}}\right)^{\frac{1-\delta}{\delta-2}}$$

where $B = 3c^2$.
For the flat universe case, the differential equation in the

$$\Omega'_{de} = 2\Omega_{de}\left(1-\Omega_{de}\right)\left(\frac{B\sqrt{\Omega_{de}}}{A^{3/2}}\sqrt{\frac{A+B}{2c^2}} - \frac{A+B}{A} + \frac{5}{2}\right), \text{ Kaniadakis model.} \tag{5.7}$$

where

$$A = \frac{3e^{-3x}H_0^2\Omega_{m,0}\Omega_{de}}{1-\Omega_{de}}$$
$$B = \sqrt{A^2 - 12c^2K^2M_p^4}.$$

We can solve the above differential equations and various values of the parameters in each model using the odeint method in Python, and compare with the datapoints of $H(z)$. In addition, this is useful for later defining our parameter priors in each model.
First, notice that in the equation (5.3)

$$\omega_l \Omega_l = \omega_m \Omega_m + \omega_r \Omega_r = \frac{1}{3}\Omega_{r,0}(z+1)^4,$$

due to $\omega_m = 0$. furthermore, notice that for plot the $H(z)$, the dark energy density can be expressed as $\rho_{de} = \Omega_{de}\rho_c = \Omega_{de} 3H^2 M_p^2$. Thus from the Friedmann equation we have

$$H^2(z) = \frac{1}{3M_p^2}\left(\rho_{r,0}(1+z)^4 + \rho_{m,0}(z+1)^3 + \rho_{de}(z)\right)$$
$$H^2(z)\left(1 - \Omega_{de}(z)\right) = \frac{H_0^2}{3M_p^2 H_0^2}\left(\rho_{r,0}(1+z)^4 + \rho_{m,0}(z+1)^3\right)$$

$$H(z) = H_0 \left(\frac{\Omega_{r,0}(1+z)^4 + \Omega_{m,0}(1+z)^3}{1 - \Omega_{de}(z)}\right)^{1/2} \tag{5.8}$$

In this equation, the dark energy parameter density $\Omega(z)$, is the solution of the differential equation in each holographic model.

5.1.1 Standard Holographic Dark Energy Model

For the first case, we get the following figures

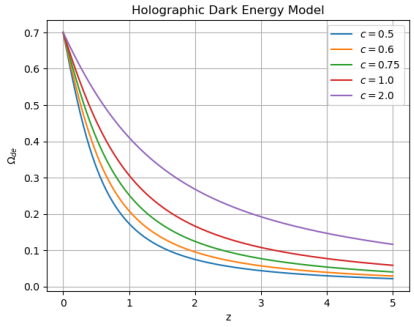

(a)

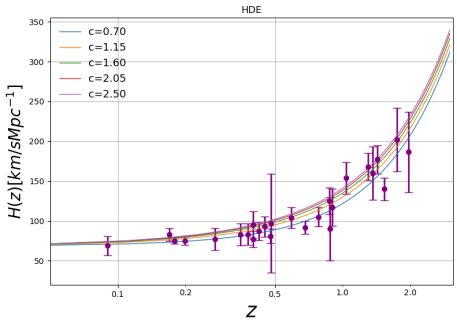

(b)

Figure 5.1: **(a)** Dark Energy density for the holographic dark energy model. **(b)** The variation of $H(z)$ with redshift z, in units when $M_p^2 = 1$ and $H_0 = 70$. In order to be consistent with data, we use the initial condition $\Omega_{de}(z = 0) = 0.7$. The bars represent the 26 $H(z)$ datapoints.

Based on these priors we find the following confidence regions

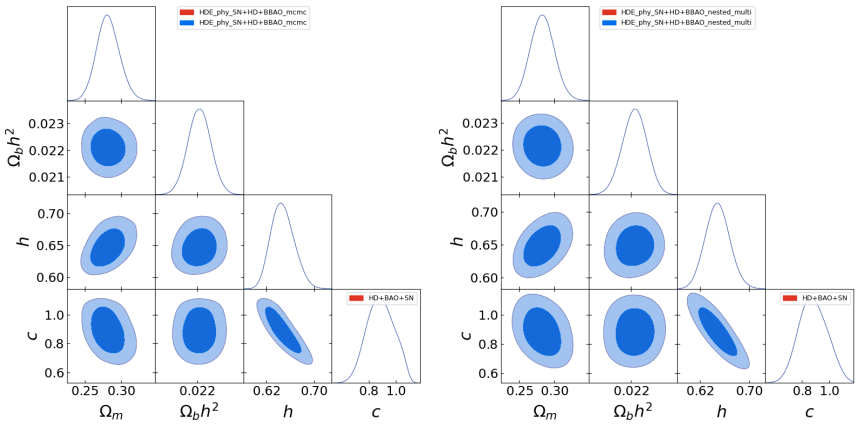

(a) (b)

Figure 5.2: **(a)** Confidence regions for the standard holographic dark energy model using MCMC. **(b)** Confidence regions for the standard holographic dark energy model using Nested Sampling with 800 live points.

5.1.2 Barrow Holographic Dark Energy

Notice that from figure (b) we can see that the value $\mathcal{B} = 0.1$ is far from the region of the data points, thus, we can discard values $\mathcal{B} < 0.1$. In addition, notice that the values in the region $0.82 \leq \mathcal{B} \leq 3$, it looks like the best fit to the data points, so it is ideal to explore in this area during parameter inference, for the case of $\mathcal{B}$. In special, we can see that for $c = 1.0$ looks like the best fit among all the solutions.
We can do the same process for the other models as in the previous case. For the Barrow model and fixing the parameter $c = 1.0$, the figures are as follows

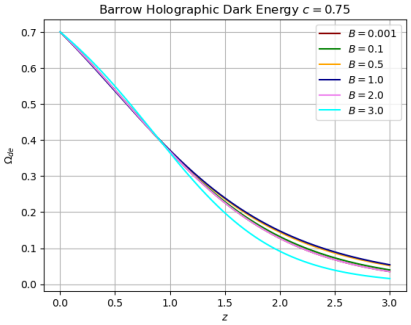

(a)

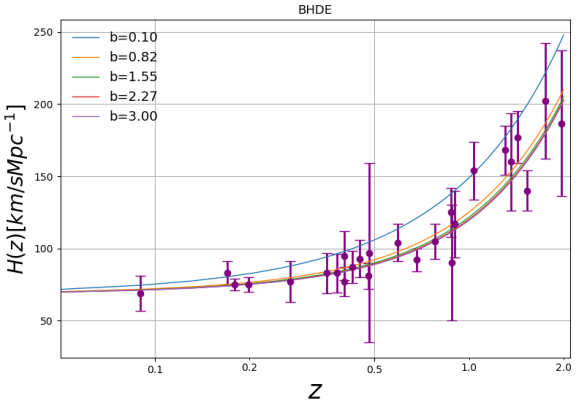

(b)

Figure 5.3: **(a)** Dark Energy density for the holographic dark energy model. **(b)** The variation of $H(z)$ with redshift z, in units when $M_p^2 = 1$ and $H_0 = 70$. In order to be consistent with data, we use the initial condition $\Omega_{de}(z = 0) = 0.7$. The bars represent the 26 $H(z)$ datapoints.

From the rigure **(a)**, notice that for the value $\mathcal{B} = 3.0$, it is far removed from

the other solutions and has a different behavior than the other solutions, so we can consider $\mathcal{B} > 2.5$ disposable values.

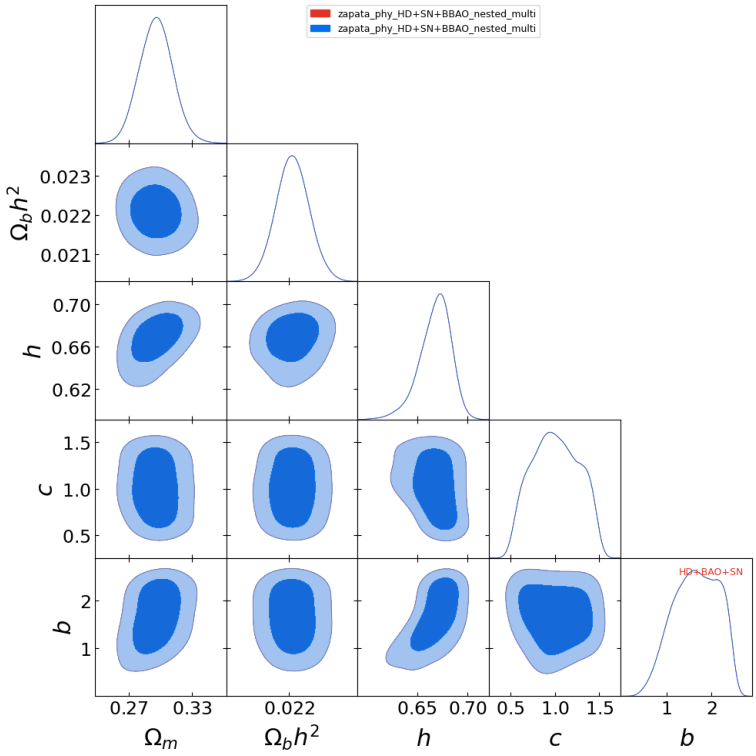

Figure 5.4: Confidence regions for the Barrow holographic dark energy model

5.1.3 Tsallis holographic dark energy

For el case of Tsallis Holographic Dark Energy Model, since we have two free parameters at the beginning, at this point we must set one of them ($c = 0.75$) and vary the other (δ), then do the same with the first set value. We obtain the following figures From these figures we can see that the $\delta = 3.67$ is outside

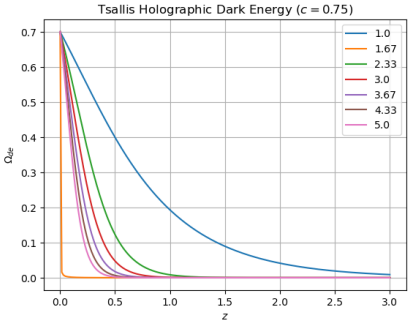

(a)

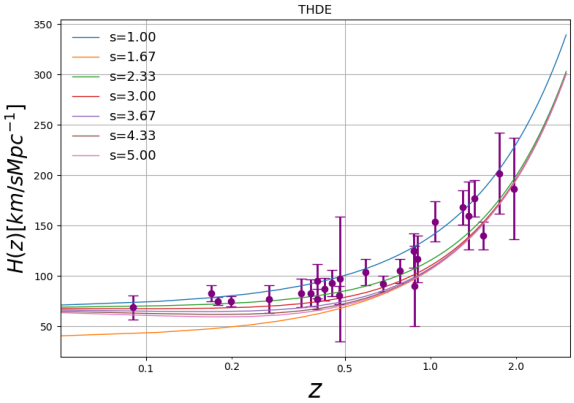

(b)

Figure 5.5: **(a)** Dark Energy density for the holographic dark energy model. **(b)** The variation of $H(z)$ with redshift z, in units when $M_p^2 = 1$ and $H_0 = 70$. In order to be consistent with data, we use the initial condition $\Omega_{de}(z = 0) = 0.7$. The bars represent the 26 $H(z)$ datapoints.

the data region of $H(z)$ for low redshifts, so we can consider $\delta \geq 3$ discardable values. On the other hand, we can see that the values closest to ΛCDM are $\delta = 1.0$, so we can consider exploring the region $1.0 \leq \delta \leq 3.0$.

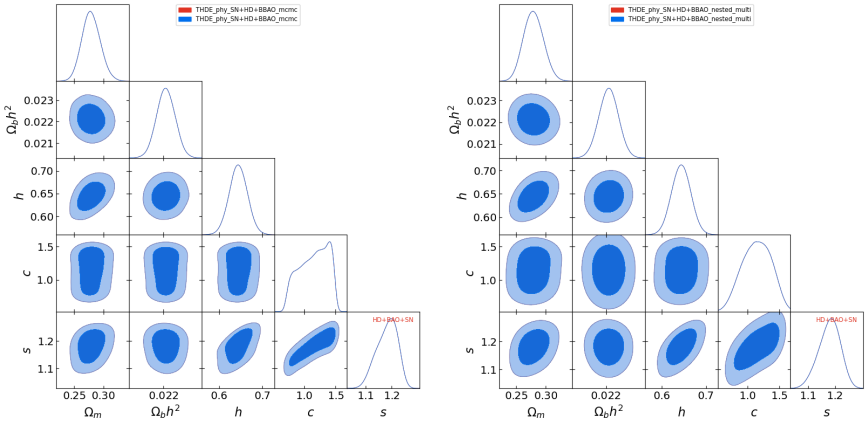

(a) (b)

Figure 5.6: **(a)** Confidence regions for the standard holographic dark energy model using MCMC. **(b)** Confidence regions for the standard holographic dark energy model using Nested Sampling with 800 live points.

5.1.4 Kaniadakis holographic dark energy

5.1.5 Parameter values

Estos valores fueron los encontrados con Nested Sampling.

Parameters				
Models	c	$\mathcal{B}$	δ	B
HDE	0.8814 ± 0.1012	-	-	-
LCDM		-	-	-
$\mathcal{T}$HDE	1.1480 ± 0.2210	-	1.1804 ± 0.0395	
$\mathcal{B}$HDE	1.0105 ± 0.2634	1.6636 ± 0.4912	-	-
$\mathcal{K}$HDE	-	-	-	-
Propuesta	-	-	-	- -

Parameters			
Models	h	Ω_m	$\Omega_b h^2$
HDE	0.6484 ± 0.0192	0.2826 ± 0.0165	0.0221 ± 0.0005
ΛCDM	0.6856 ± 0.0062	0.2977 ± 0.0077	0.0224 ± 0.0003
$\mathcal{T}$HDE	0.6443 ± 0.0208	0.2792 ± 0.0162	0.0221 ± 0.0005
$\mathcal{B}$HDE	0.6678 ± 0.0159	0.2961 ± 0.0157	0.0221 ± 0.0005
$\mathcal{K}$HDE	-	-	-
Propuesta	-	-	-

Models	AIC	ΔAIC	$Log(\mathcal{Z})$	GR	χ^2
LCDM	67.2544	0		0.1826495570437323	61.2544
HDE	70.8117	3.33	-39.0454 ± 0.2614	0.1318843394625583	62.8118
$\mathcal{B}$HDE	72.1876	4.08	-37.9168 ± 0.1203	0.09339875908851569	60.6798
$\mathcal{T}$HDE	76.0228	5.40	-40.6392 ± 0.2714	0.09923644880083493	63.4644

Appendices

Bibliography

[] "ESA Science & Technology - Hubble image of variable star RS Puppis". en. In: (). Accessed: 2024-2-22.

[Aur+21] Aurich, R. et al. "The variance of the CMB temperature gradient: a new signature of a multiply connected Universe". In: (June 2021).

[Bar20] Barrow, J. D. "The Area of a Rough Black Hole". In: *Phys. Lett. B* vol. 808 (2020), p. 135643. arXiv: 2004.09444 [gr-qc].

[Hsu04] Hsu, S. D. "Entropy bounds and dark energy". In: *Physics Letters B* vol. 594, no. 1 (2004), pp. 13–16.

[KS23] Kord Zangeneh, M. and Sheykhi, A. "Modified cosmology through Kaniadakis entropy". In: (Nov. 2023). arXiv: 2311.01969 [gr-qc].

[Li04] Li, M. "A model of holographic dark energy". In: *Physics Letters B* vol. 603, no. 1 (2004), pp. 1–5.

[Lid98] Liddle, A. R. *An introduction to modern cosmology*. 1998.

[NF22] Nojiri, S. and Faraoni, V. *How fundamental is entropy? From non-extensive statistics and black hole physics to the holographic dark universe*. Jan. 2022.

[PB22] Pathria, R. and Beale, P. D. "9 - Thermodynamics of the early universe". In: *Statistical Mechanics (Fourth Edition)*. Ed. by Pathria, R. and Beale, P. D. Fourth Edition. Academic Press, 2022, pp. 291–313.

[Pee93] Peebles, P. J. E. *Principles of physical cosmology*. Vol. 27. Princeton university press, 1993.

[Per00] Perlmutter, S. "Supernovae, dark energy, and the accelerating universe: The Status of the cosmological parameters". In: *Int. J. Mod. Phys. A* vol. 15S1 (2000). Ed. by Jaros, J. and Peskin, M. E., pp. 715–739.

[Pla+20] Planck Collaboration et al. "Planck 2018 results - VI. Cosmological parameters". In: *A&A* vol. 641 (2020), A6.

[RV18] Ramos-Sanchez, S. and Vidal, O. *Relatividad para futuros fisicos*. Textos contemporaneos. Copit-Arxives, 2018.

[Sar+18] Saridakis, E. N. et al. "Holographic dark energy through Tsallis entropy". In: *Journal of Cosmology and Astroparticle Physics* vol. 2018, no. 12 (Dec. 2018), p. 012.

[Tsa88] Tsallis, C. "Possible generalization of Boltzmann-Gibbs statistics". In: *Journal of Statistical Physics* vol. 52 (July 1988), pp. 479–487.